Classification of ^{20}F states below 4.4 MeV

H. T. Fortune
Department of Physics and Astronomy, University of Pennsylvania, Philadelphia, Pennsylvania, 19104

(Received 10 May 2018; published 11 July 2018)

Angle-integrated cross sections and forward/backward ratios for the reaction ^{18}O(^{3}He, p)^{20}F have been combined with existing information in order to classify ^{20}F states up to 4.4 MeV excitation. Experimental counterparts are now known for all 13 $(sd)^4$ shell-model states in this region.

DOI: 10.1103/PhysRevC.98.014314

I. INTRODUCTION AND HISTORY

Many different reactions have been used to investigate ^{20}F [1]. These include ^{19}F(d,p) [2–4], ^{19}F($d,p\gamma$) [5,6], ^{19}F(n,γ) [7–11], ^{18}O(^{3}He, p) [12–14], ^{18}O(^{3}He, $p\gamma$) [5,15–17], ^{18}O($t,n\gamma$) [18], ^{16}O(^{7}Li,^{3}He) [19], ^{14}N(^{7}Li, p) [20,21], and ^{13}C(^{11}B,α) [22,23]. Others are β decay of ^{20}O [24], ^{20}Ne(n,p) [25], ^{20}Ne(t,^{3}He) [26,27], ^{21}Ne(d,^{3}He) [28], ^{21}Ne(t,α) [29], and ^{22}Ne(p,^{3}He) [30]. Below about 4.6 MeV [31], all ^{20}F states can be characterized as belonging primarily to one of three different configurations: positive-parity $(sd)^4$, negative-parity $(sd)^5(1p)^{-1}$, and positive-parity $(sd)^6(1p)^{-2}$. In the language of weak coupling, the five-particle one-hole (5p-1h) states are ^{21}Ne $\otimes$ ^{15}N, and the 6p-2h states are ^{22}Ne $\otimes$ ^{14}N. States of the form ^{22}Na $\otimes$ ^{14}C are expected above about 5.1 MeV [31]. Population of these different configurations will be quite different in different reactions. For example, in the ^{18}O(^{3}He, p) reaction, most $(sd)^4$ states should be strong. (But, see exceptions below.) In a direct (^{3}He, p) reaction, the nucleons in the target are unchanged as an np pair is transferred from the projectile to the target. Thus, states that are directly populated should have nonzero overlap with the ground state (g.s.) of ^{18}O. Therefore the 5p-1h states can be made through the 4p-2h component of ^{18}O(g.s.) [32], whereas population of the 6p-2h states would be forbidden. (The core excitation in ^{18}O is mostly ^{20}Ne $\otimes$ ^{14}C.) But, they can acquire strength by mixing with nearby $(sd)^4$ states.

Sometimes, combining results of two or more reactions can be useful in pinning down the characteristics of a particular state. For example, the ^{14}N(^{7}Li, p) reaction determined that the 2.97-MeV "state" was actually a closely spaced doublet [21]. It was suggested that the unknown member was probably the 4^- state expected near this energy. The ^{13}C(^{11}B,α) reaction [22] was used to populate the doublet, and the γ decays were observed [23]. The unknown member was confirmed, and its γ decays were only to the lowest 4^+ and 3^- states. This state still has a tentative (4^-) assignment in the latest compilation. Except for it and two (3^-) states, all levels below 3 MeV now have unique J^π assignments [1].

The 3^+ member of the 2.97-MeV doublet is almost certainly the mirror of the ^{20}Na state at 2.65 MeV that is important for the ^{19}Ne(p,γ) reaction in stellar burning [33–35]. Its reasonably large mirror energy difference has been attributed [33] to the presence in its wave function of an appreciable $2s_{1/2}$ nucleon component coupled to an excited state.

In the reaction ^{18}O(^{3}He, p)^{20}F, all final states below 6.5 MeV have isospin equal to unity [1]. Selection rules allow spin and isospin transfer ST of 01 and/or 10. Natural-parity states are populated with $L = J$, $S = 0$ and 1; unnatural-parity with $L = J \pm 1$, $S = 1$. For $(sd)^4$ final states, L is limited to $L = 0,2,4$; low-lying negative-parity intruder states are reached via $L = 1$ and 3. Earlier, we investigated this reaction at $E(^3\text{He}) = 18$ [12] and 19 [13] MeV. Angular distributions at 18 MeV [12] were analyzed with distorted-wave Born-approximation (DWBA) calculations using two-nucleon transfer amplitudes from a shell-model calculation. Comparisons between experimental data and calculations allowed identification of several states whose dominant structure was $(sd)^4$.

Combining results of ^{19}F(d,p) [3,5] and ^{18}O(^{3}He, p) [12,13] confirmed J^π of 1^+ and 0^+ for states at 3.488 and 3.526 MeV, respectively, even though the latest compilation still lists the latter as tentative [1]. In the ^{18}O(^{3}He, p) reaction, observation of $L = 0 + 2$ angular distributions suggested assignments of (1^+) for states at 3.17, 3.966, and 4.082 MeV [13]. Comparison with $(sd)^4$ shell-model calculations suggests that these three states all are of core-excited character. It was suggested that the 3.17-MeV state is dominantly ^{22}Ne(g.s.) $\otimes$ ^{14}N(g.s.) [13]. The present aim is to attempt to classify other states.

II. RESULTS AND ANALYSIS

The experimental procedure was the same as the one used previously [13]. The beam energy was 19.0 MeV. The target was a gold-backed foil of an oxide of tungsten, prepared by heating a tungsten filament in oxygen gas that was enriched to 98% in ^{18}O. Because of some uncertainty concerning the ^{18}O content of the target, an additional exposure was taken with a gas target to obtain an absolute cross-section scale. Outgoing protons were momentum analyzed in a multiangle spectrograph and detected on photographic plates in the focal planes. Data were collected simultaneously at 22 angles from 7.5 to 172.5 degrees, in steps of 7.5 degrees, for all states up to $E_x = 4.4$ MeV.

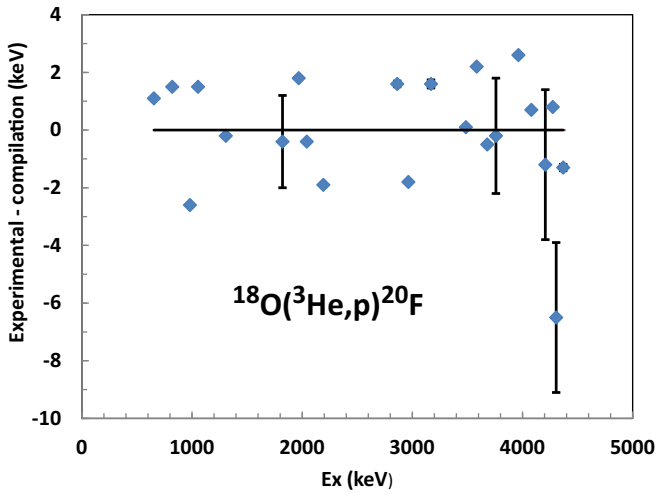

FIG. 1. Differences between present excitation energies and those from the compilation [1] are plotted vs excitation energy. Uncertainties from the compilation are displayed whenever they are larger than the data points. The rms average of the difference is 1.3 keV.

The latest compilation [1] lists 29 states in this region of excitation energy. In the present data, six pairs of states are unresolved doublets, so that 23 sets of data were obtained. Excitation energies and J^π values from the compilation are listed in Table I, along with results of the present experiment. Energy uncertainties larger than 2 keV are listed. Uncertainties for the present excitation energies are the standard deviations of energies extracted at 22 angles. They average 3.1 keV. However, the root-mean-square (rms) deviation between present and compiled energies is only 1.3 keV. (For this computation, I have removed the 4.31-MeV state, which has a large discrepancy and a large uncertainty.) A plot of the differences is given in Fig. 1.

For the doublets, the present energies suggest that in most cases only one member of the doublet is populated significantly in the present experiment. For the 1.8-MeV doublet, the separation is 20 keV, but the present energy agrees with that of the 5^+ member to within 0.4 keV. Of course, in some cases, the doublet separation is too small for such a conclusion [e.g., 2.97 MeV, separation 2 keV; 4.2 MeV, separation 9(4) keV]. I have divided the states into three distinct categories: (1) known sd-shell states, (2) states that are known not to be sd shell (e.g., negative-parity states), and (3) other. For reasons that will become clear shortly, two of the sd-shell states are labeled "weak sd."

Angular distributions have been integrated over 0–90 and 90–180 degrees. Results are listed in Table I. It is to be expected that states that are reached by direct two-nucleon transfer will have more cross section at forward angles [36]. Figure 2 plots the forward/backward ratio vs excitation energy. Data for different classes of states have been plotted with different symbols. Except for the two weak sd states, it can be seen that all the sd-shell states exhibit larger forward/backward ratios than any of the other or non-sd states.

The two weak sd-shell states are the 2^+ ground state (g.s.) and the 4^+ state at 0.824 MeV. The $K = 2$ g.s. rotational

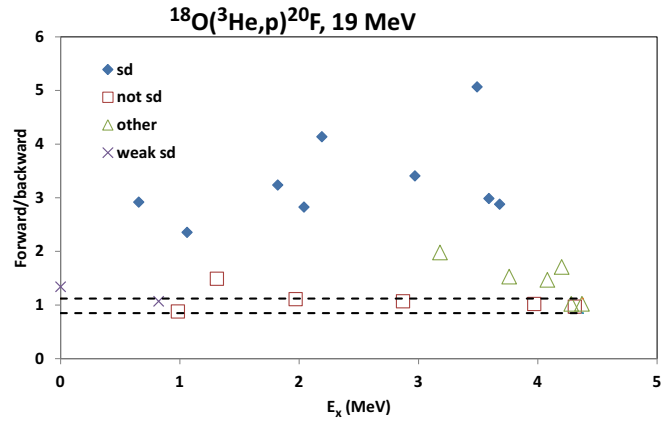

FIG. 2. Ratio of forward (0–90 degrees)/backward (90–180 degrees) cross sections for the reaction ^{18}O(^{3}He, p)^{20}F is plotted vs excitation energy. The dashed band encompasses levels with $f/b \sim 1$.

band is dominated by the quantum numbers $K_L = 1$, $K_S = 1$, $K = 2$ [37]. Thus, the 2^+ and 4^+ states are primarily $L = 1$ and 3, respectively, with $S = 1$. Such a configuration would not be expected to be populated in direct two-nucleon transfer. However, some component of $L = 2$ and 4 is also present. In the earlier comparison [12] with $(sd)^4$ shell-model calculations, these two states were predicted to be weak, but they were even weaker than predicted by the shell model. Ratios of experimental to DWBA cross sections, using $2n$ transfer amplitudes from the shell model, are plotted in Fig. 3 for seven $(sd)^4$ states [12]. The 0^+ state at 3.52 MeV is too weak to be observed. It is far enough away (38 keV) from the 1^+ state at 3.49 MeV that it would have been seen if it had been populated appreciably. Presumably, its structure is mostly $L = 1$, $S = 1$.

The large forward/backward enhancement for sd-shell states is also apparent in a plot (Fig. 4) that compares this ratio

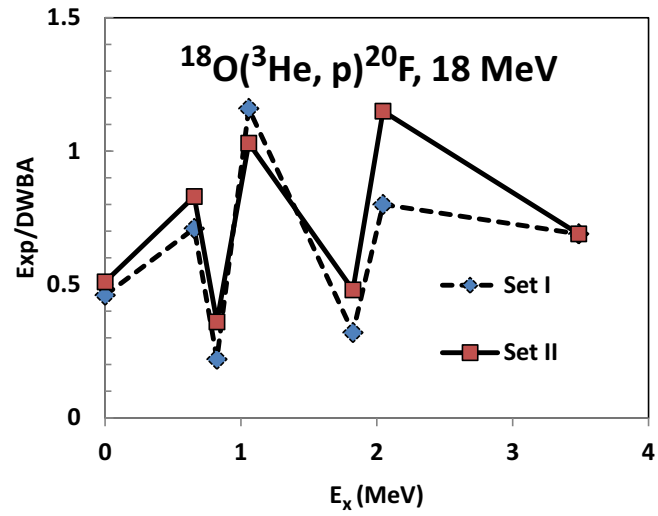

FIG. 3. From Ref. [12], the ratio of experimental to DWBA cross sections vs excitation energy for seven sd-shell states. Set I and Set II refer to different optical-model potentials [12].

TABLE I. Excitation energies (keV), J^π, and cross sections for the reaction ^{18}O(^{3}He, p)^{20}F. Superscript labels denote level classifications from Ref. [12] and the present work: *sd* for *sd*-shell states, *n* for non-*sd*, and *w* for weak *sd*.

Compilation[a]		Present		Total cross sections (μb)							
E_x	J^π	E_x	ΔE_x	0–90	Unc.	90–180	Unc.	0–180	Unc.	f/b[b]	$\Delta(f/b)$
0^w	2^+	0	3.1	392	14	293	13	685	19	1.34	0.08
656.0^{sd}	3^+	657.1	3.2	1010	20	346	13	1356	24	2.92	0.12
822.7^w	4^+	824.2	3.4	456	16	426	15	882	22	1.07	0.05
983.6^n	1^-	981	2.0	51	5	58	5	109	7	0.88	0.11
1056.8^{sd}	1^+	1058.3	2.8	431	14	183	9	614	17	2.36	0.14
1309.2^n	2^-	1309	3.1	167	9	112	7	279	11	1.49	0.12
1823.8^{sd}	5^+	1823.4	3.7	2370	40	732	20	3102	45	3.24	0.10
1843.8^n	2^-										
1970.8^n	3^-	1972.6	4.6	233	10	210	10	443	14	1.11	0.07
2044^{sd}	2^+	2043.6	4.5	424	14	150	8	574	16	2.83	0.18
2194.3^{sd}	3^+	2192.4	3.3	1560	30	377	14	1937	33	4.14	0.17
2864.9^n	3^-	2866.5	2.7	153	18	143	9	296	20	1.07	0.14
2966.1^{sd}	3^+	2964.3	3.0	1830	30	537	17	2367	34	3.41	0.12
2968^n	(4^-)										
3171.7	$1^+,0^-$	3173.3	3.0	234	19	118	7	352	20	1.98	0.20
3488.4^{sd}	1^+	3488.5	3.0	2630	60	519	16	3149	62	5.07	0.19
3526.3^w	(0^+)										
3586.5^{sd}	(2)	3588.7	3.0	1780	50	596	19	2376	53	2.99	0.13
3589.8^{sd}	(3)										
$3669(3)^{sd}$	(4^+)										
3680.2	(2)	3679.7	3.0	599	20	208	13	807	24	2.88	0.20
3761	$(\geqslant 3)$	3760.8	2.9	346	13	226	13	572	18	1.53	0.11
3965.1^n	(1^+)	3967.7	3.1	134	8	132	10	266	13	1.02	0.10
4082.2	(1^+)	4082.9	3.1	230	11	156	9	386	14	1.47	0.11
4199.3(2.7)	$\geqslant 3$										
4208.1(2.7)	$\geqslant 3$	4206.9	2.7	428	14	251	14	679	20	1.71	0.11
4277.1	$1^+,2^+$	4277.9	3.0	189	10	185	12	374	16	1.02	0.09
4312.0(2.6)	(0^+)	4305.5	3.1	148	11	152	13	300	17	0.97	0.11
4371.5		4370.2	3.1	90	13	88	9	178	16	1.02	0.18

[a]From Ref. [1]. Uncertainties larger than 2 keV are listed.
[b]Ratio of forward/backward cross sections.

with the quantities $\sigma_{\rm tot}/(2J+1)$. In this plot (and in Fig. 2), eight states are clustered around $f/b = 1.0$. A dashed band in Fig. 2 encompasses these states. One is the 4^+ second-excited state discussed earlier. These are listed in Table II and their results are plotted in Fig. 5. These are thus good candidates for states with little or no direct transfer. It would thus appear that the three states near 4 MeV that are thought to have positive parity, 3.97 (1^+), 4.28 1^+, 2^+, and 4.31 (0^+) MeV, have very small *sd*-shell components.

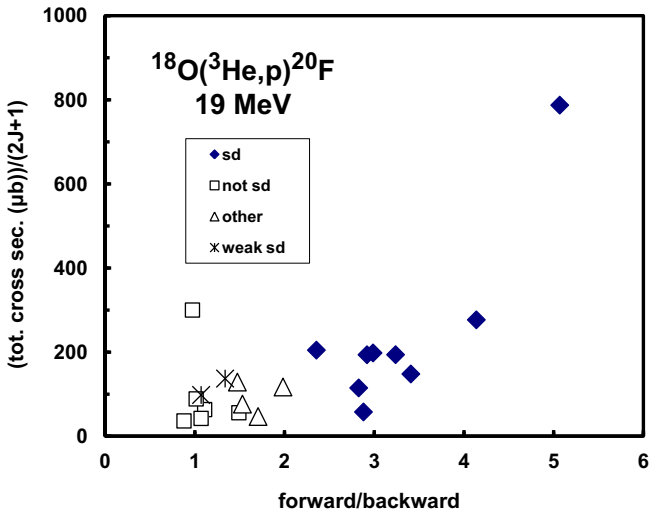

FIG. 4. Total cross sections (0–180 degrees) divided by $2J+1$ are plotted vs forward/backward ratios.

TABLE II. States with approximately symmetric angular distributions in the reaction ^{18}O(^{3}He, p)^{20}F.

E_x (MeV)	J^π	f/b	$\Delta(f/b)$	Total (μb)	Unc (μb)	tot/$(2J+1)$
0.822	4^+	1.07	0.05	882	22	98.0
0.983	1^-	0.88	0.11	109	7	36.3
1.97	3^-	1.11	0.07	443	14	63.3
2.87	3^-	1.07	0.14	296	20	42.3
3.97	(1^+)	1.02	0.10	266	13	(88.7)
4.28	$1^+,2^+$	1.02	0.09	374	16	
4.31	(0^+)	0.97	0.11	300	17	
4.37		1.02	0.18	178	16	

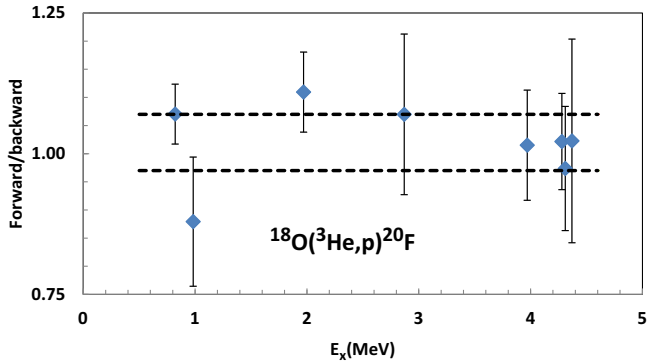

FIG. 5. Forward/backward ratios for six states (listed in Table II) that have a small direct component.

The large f/b enhancement for sd-shell states is present for all J values, as can be seen in Fig. 6, where the abscissa is $2J+1$. For this plot, I have summed the $(2J+1)$'s for doublets.

The left-hand column of Fig. 7 contains all the $(sd)^4$ shell-model states up to 3.8 MeV [31]. The theoretical spectrum has a large gap just above 3.8 MeV. The next shell-model state is 7^+ at 4.458 MeV, and the next 1^+ theoretical state is at 4.882 MeV. The right-hand column lists all the experimental states that were assigned $(sd)^4$ character by [12] and those from the present work with large f/b ratios. The close correspondence between shell-model and experimental states is remarkable. For the first nine excited states, the average of shell model minus experimental energy is –47 keV, and the root-mean-square (rms) deviation is 75 keV. Other than the well-known 1^+ and 0^+ states, the shell model has three states in the region 3.3–3.8 MeV, with $J^\pi = 2, 3$, and 4. In this region, the experiment shows two large f/b ratios, for the 3.59- and 3.68-MeV doublets. It is thus likely that one of these doublets contains two $(sd)^4$ states and the other only one.

A state at 3.59 MeV has a large $\ell = 2$ spectroscopic factor in ^{19}F(d,p) : $(2J+1)S(2) = 0.38$ and 0.42 at 12 [3] and 16 [5] MeV, respectively. (The entry of 0.038 in Table 20.15 of Ref. [1] is in error.) In the earlier ^{18}O$(^3$He$,p)$ work [12], the angular distribution was reported as $L = 2+4$. These results are consistent with $J^\pi = 3^+$ for a single state. However, the

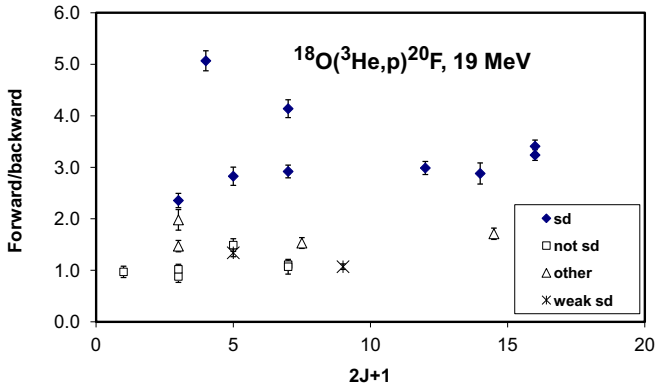

FIG. 6. Forward/backward ratios plotted vs $2J+1$.

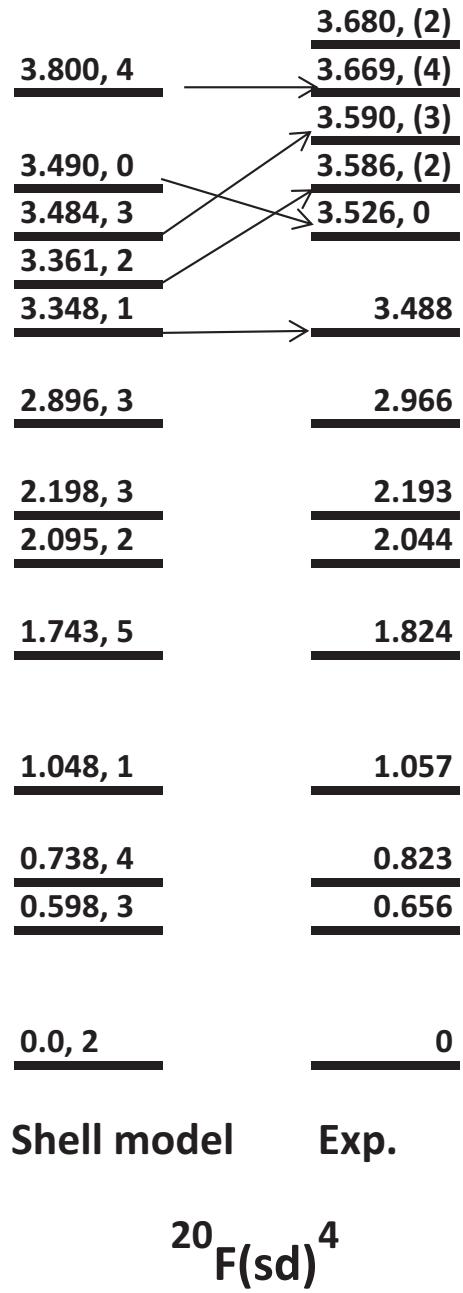

FIG. 7. The left-hand column contains all the $(sd)^4$ shell-model states up to 3.8 MeV [31], listed by excitation energy and J. The right-hand column contains experimental states identified as $(sd)^4$ by Ref. [12] and herein.

^{14}N$(^7$Li$,p)$ results indicated preference for a doublet, because the total cross section was 4σ larger than that expected for a 3^+ state [21]. And, indeed, the doublet nature is now firm [1]. In the ^{22}Ne(d,α) reaction [34], the 3.59-MeV state was too strong to be identified with either the 2^+ or 3^+ model state, but it could correspond to both.

The ^{14}N$(^7$Li$,p)$ paper [21] also suggested that the 3.68-MeV state was a doublet, as it turned out to be [1]. The ^{22}Ne(d,α) paper [38] reported that the cross section for the 3.68-MeV state was consistent with it being identified with the

second 4^+ model state. Thus, the most likely outcome is that the 3.59-MeV doublet contains both the 2^+ and 3^+ shell-model states expected in this region, and the 3.68-MeV doublet contains the 4^+ shell-model state and a non-sd state. If this is correct, γ decays [1] favor 2^+ for the lower member of the 3.59-MeV doublet and 3^+ for the higher member. At 3.68 MeV, the lower member decays only to the 2^+ g.s., whereas the other has several decays to states with $J^\pi = 2^+, 3^+, 1^+$, and 2^- [1], strongly favoring the lower member as the 4^+ state.

Because of the large gap in the theoretical spectrum, it is likely that all the other experimental states in the 4-MeV region are of non-sd character. These classifications are consistent with information from several different reactions. For the state at 4.37 MeV, its ^{14}N(^{7}Li, p) cross section [21] was so small as to require $J = 0$. A preference for 0^- was based on weak-coupling considerations. Because they are observed with direct-reaction characteristics in both (d, p) [3–5] and (^{3}He, p) [12,13], positive-parity states at 3.97, 4.08, 4.28, and 4.32 MeV clearly contain some $(sd)^4$ component, but it is not dominant. The 3.76-MeV state and both members of the 4.20-MeV doublet have $J \geqslant 3$, and are good candidates to have negative parity.

III. SUMMARY

I have evaluated angle-integrated cross sections and forward/backward ratios for 23 angular distributions in the reaction ^{18}O(^{3}He, p)^{20}F. Results have been combined with existing information from a variety of reactions in order to classify ^{20}F states below 4.4 MeV in excitation. Experimental counterparts are now known for all 13 $(sd)^4$ shell-model states in this region.

[1] D. R. Tilley, C. M. Cheves, J. H. Kelley, S. Raman, and H. R. Weller, Nucl. Phys. **636**, 249 (1998).
[2] H. T. Fortune, G. C. Morrison, R. C. Bearse, J. L. Yntema, and B. H. Wildenthal, Phys. Rev. C **6**, 21 (1972).
[3] H. T. Fortune and R. R. Betts, Phys. Rev. C **10**, 1292 (1974).
[4] C. A. Mosley, Jr. and H. T. Fortune, Phys. Rev. C **16**, 1697 (1977).
[5] P. R. Chagnon, Nucl. Phys. **59**, 257 (1964).
[6] T. Holtebekk, S. Tryti, and G. Vamraak, Nucl. Phys. A **134**, 353 (1969).
[7] E. G. Nadjakov, Nucl. Phys. **48**, 492 (1963).
[8] I. Berquist, J. A. Biggerstaff, J. H. Gibbons, and W. M. Good, Phys. Rev. **158**, 1049 (1967).
[9] H. Spilling, H. Gruppelaar, H. F. de Vries, and A. M. J. Spits, Nucl. Phys. A **113**, 395 (1968).
[10] R. Hardell and A. Hasselgren, Nucl. Phys. A **123**, 215 (1969).
[11] S. Raman, E. K. Warburton, J. W. Starner, E. T. Jurney, J. E. Lynn, P. Tikkanen, and J. Keinonen, Phys. Rev. C **53**, 616 (1996).
[12] D. J. Crozier and H. T. Fortune, Phys. Rev. C **10**, 1697 (1974).
[13] R. Medoff, L. R. Medsker, S. C. Headley, and H. T. Fortune, Phys. Rev. C **14**, 1 (1976).
[14] M. S. Chowdhury, M. A. Zaman, and H. M. Sen Gupta, Phys. Rev. C **46**, 2273 (1992).
[15] G. A. Bissinger, R. M. Mueller, P. A. Quin, and P. R. Chagnon, Nucl. Phys. A **90**, 1 (1967).
[16] P. A. Quin, A. A. Rollefson, G. A. Bissinger, C. P. Browne, and P. R. Chagnon, Phys. Rev. **157**, 991 (1967).
[17] P. A. Quin, G. A. Bissinger, and P. R. Chagnon, Nucl. Phys. A **155**, 495 (1970).
[18] J. G. Pronko and R. W. Nightingale, Phys. Rev. C **4**, 1023 (1971).
[19] H. T. Fortune and J. N. Bishop, Nucl. Phys. A **304**, 221 (1978).
[20] J. N. Bishop and H. T. Fortune, Phys. Rev. Lett. **34**, 1350 (1975).
[21] H. T. Fortune and J. N. Bishop, Nucl. Phys. A **293**, 221 (1977).
[22] G.-B. Liu and H. T. Fortune, Phys. Rev. C **38**, 2134 (1988).
[23] J. C. Legg, D. J. Crozier, G. G. Seaman, and H. T. Fortune, Phys. Rev. C **18**, 2202 (1978).
[24] D. E. Alburger, G. Wang, and E. K. Warburton, Phys. Rev. C **35**, 1479 (1987).
[25] B. W. Pointon, O. Häusser, R. Henderson, A. Celler, K. Hicks, K. P. Jackson, R. Jeppesen, B. Larson, J. Mildenberger, A. Trudel, M. Vetterli, and S. Yen, Phys. Rev. C **44**, 2430 (1991).
[26] N. M. Clarke, P. R. Hayes, M. B. Becha, C. N. Pinder and S. Roman, J. Phys. G **16**, 1547 (1990).
[27] N. M. Clarke, S. Roman, C. N. Pinder and P. R. Hayes, J Phys. G **19**, 1411 (1993).
[28] G. F. Millington, J. R. Leslie, W. Mclathie, G. C. Ball, W. G. Davies, and J. S. Foster, Nucl. Phys. A **228**, 382 (1974).
[29] G.-B. Liu and H. T. Fortune, Phys. Rev. C **37**, 1818 (1988).
[30] J. C. Hardy, H. Brunnader, and Joseph Cerny, Phys. Rev. Lett. **22**, 1439 (1969).
[31] H. T. Fortune and B. H. Wildenthal, Phys. Rev. C **30**, 1063 (1984).
[32] R. L. Lawson, F. J. D. Serduke, and H. T. Fortune, Phys. Rev. C **14**, 1245 (1976).
[33] H. T. Fortune, R. Sherr, and B. A. Brown, Phys. Rev. C **61**, 057303 (2000).
[34] J. P. Wallace *et al.*, Phys. Lett. B **712**, 59 (2012).
[35] J. P. Wallace and P. J. Woods, Phys. Rev. C **86**, 068801 (2012).
[36] N. Austern, *Direct nuclear reaction theories*, (John Wiley, New York, 1970).
[37] D. J. Millener (private communication).
[38] H. T. Fortune and J. D. Garrett, Phys. Rev. C **14**, 1695 (1976).